

Published in final edited form as:

*Cell Metab.* 2012 August 8; 16(2): 189–201. doi:10.1016/j.cmet.2012.06.013.

## Inhibiting Adipose Tissue Lipogenesis Reprograms Thermogenesis and PPAR $\gamma$ Activation to Decrease Diet-induced Obesity

Irfan J. Lodhi<sup>1</sup>, Li Yin<sup>1</sup>, Anne P. L. Jensen-Urstad<sup>1</sup>, Katsuhiko Funai<sup>1</sup>, Trey Coleman<sup>1</sup>, John H. Baird<sup>1</sup>, Meral K. El Ramahi<sup>1</sup>, Babak Razani<sup>1,2</sup>, Haowei Song<sup>1</sup>, Fong Fu-Hsu<sup>1</sup>, John Turk<sup>1</sup>, and Clay F. Semenkovich<sup>1,3,\*</sup>

<sup>1</sup>Division of Endocrinology, Metabolism & Lipid Research, Washington University School of Medicine, St. Louis, Missouri, 63110, USA

<sup>2</sup>Cardiovascular Division, Washington University School of Medicine, St. Louis, Missouri, 63110, USA

<sup>3</sup>Department of Cell Biology and Physiology, Washington University School of Medicine, St. Louis, Missouri, 63110, USA

### SUMMARY

De novo lipogenesis in adipocytes, especially with high fat feeding, is poorly understood. We demonstrate that an adipocyte lipogenic pathway encompassing fatty acid synthase (FAS) and PexRAP (Peroxisomal Reductase Activating PPAR $\gamma$ ) modulates endogenous PPAR $\gamma$  activation and adiposity. Mice lacking FAS in adult adipose tissue manifested increased energy expenditure, increased brown fat-like adipocytes in subcutaneous adipose tissue, and resistance to diet-induced obesity. FAS knockdown in embryonic fibroblasts decreased PPAR $\gamma$  transcriptional activity and adipogenesis. FAS-dependent alkyl ether phosphatidylcholine species were associated with PPAR $\gamma$  and treatment of 3T3-L1 cells with one such ether lipid increased PPAR $\gamma$  transcriptional activity. PexRAP, a protein required for alkyl ether lipid synthesis, was associated with peroxisomes and induced during adipogenesis. PexRAP knockdown in cells decreased PPAR $\gamma$  transcriptional activity and adipogenesis. PexRAP knockdown in mice decreased expression of PPAR $\gamma$ -dependent genes and reduced diet-induced adiposity. These findings suggest that inhibiting PexRAP or related lipogenic enzymes could treat obesity and diabetes.

### INTRODUCTION

A relentless increase in mean global body weight since 1980 has resulted in an estimated 1.5 billion overweight people worldwide, of which a half billion are obese (Finucane et al., 2011). Obesity leads to diabetes, which is associated with premature death from many causes (Seshasai et al., 2011). Obesity is caused by positive energy balance leading to expansion of adipocyte mass. However, adipocytes possess functional pathways that might be targeted to complement therapies altering energy balance. De novo lipogenesis, an adipocyte function that requires the multifunctional enzyme fatty acid synthase (FAS)

© 2012 Elsevier Inc. All rights reserved

\*Correspondence: csemenko@wustl.edu.

**Publisher's Disclaimer:** This is a PDF file of an unedited manuscript that has been accepted for publication. As a service to our customers we are providing this early version of the manuscript. The manuscript will undergo copyediting, typesetting, and review of the resulting proof before it is published in its final citable form. Please note that during the production process errors may be discovered which could affect the content, and all legal disclaimers that apply to the journal pertain.

(Semenkovich, 1997), is one such potential target since adipose tissue FAS has been implicated in obesity and insulin resistance in humans (Moreno-Navarrete et al., 2009; Roberts et al., 2009; Schleinitz et al., 2011).

Fatty acid synthase catalyzes the first committed step in de novo lipogenesis. The magnitude of de novo lipogenesis is different in rodents and people. Lipogenesis is thought to be a relatively minor contributor to whole body lipid stores in a present-day human consuming a typical high fat diet (Aarsland et al., 1996; Letexier et al., 2003; McDevitt et al., 2001). However, pharmacologic or genetic manipulation of enzymes in the lipogenic pathway can have profound metabolic consequences (Postic and Girard, 2008), suggesting that de novo lipogenesis might serve a signaling function independent of the generation of lipid stores (Lodhi et al., 2011). Consistent with this concept, FAS in liver is part of a lipogenic pathway involved in the generation of a ligand for peroxisome proliferator-activated receptor  $\alpha$  (PPAR $\alpha$ ) (Chakravarthy et al., 2009), a key transcriptional regulator of fatty acid oxidation.

PPARs, consisting of PPAR $\alpha$ , PPAR $\delta$  and PPAR $\gamma$ , are ligand activated transcription factors that form obligate heterodimers with the retinoid X receptor (RXR) and regulate metabolism (Wang, 2010). Ligand binding results in a conformational change in the receptor, promoting dissociation of repressors, recruitment of co-activators, and subsequent activation of target gene expression. This nuclear receptor family was identified and named based on activation by chemicals that promote proliferation of peroxisomes (Dreyer et al., 1992; Issemann and Green, 1990).

Peroxisomes participate in the oxidation of certain fatty acids as well as the synthesis of bile acids and ether lipids (Wanders and Waterham, 2006). These single membrane-enclosed organelles are present in virtually all eukaryotic cells. In adipocytes they tend to be small and were referred to as microperoxisomes by Novikoff and colleagues, who documented a large increase in peroxisome number during the differentiation of 3T3-L1 adipocytes (Novikoff and Novikoff, 1982; Novikoff et al., 1980).

We sought to evaluate the role of de novo lipogenesis in adipocyte function and metabolism. Here we show that a lipogenic pathway encompassing FAS and PexRAP (Peroxisomal Reductase Activating PPAR $\gamma$ ), an enzyme localized to peroxisomes and encoded by a previously unidentified mammalian gene, contributes to the endogenous activation of PPAR $\gamma$  and modulates adiposity with high fat feeding.

## RESULTS

### Targeted Deletion of Adipose Tissue FAS

We generated FAS Knocked Out in Fat (FASKOF) mice by crossing FAS<sup>lox/lox</sup> mice (Chakravarthy et al., 2005) with adiponectin-Cre transgenic mice (Eguchi et al., 2011). FASKOF mice, born at the expected Mendelian frequency, were overtly normal. FAS protein was decreased in white and brown adipose tissue of FASKOF relative to Cre only (without lox sites) and lox/lox (without Cre) control mice (Figures 1A,B). FAS protein content was not decreased in whole brain extracts of FASKOF mice (Figure 1B). FAS mRNA assayed by quantitative RT-PCR was the same in the hypothalamus of FASKOF and lox/lox mice (not shown), suggesting that phenotypes are not likely to be due to CNS effects (Lu et al., 2011; Ryan et al., 2011). FAS enzyme activity was decreased in fat but not liver of FASKOF mice (Figure 1C). Hepatic FAS enzyme activity was not significantly increased in the setting of decreased adipose tissue FAS activity (Figure 1C).

Chow-fed FASKOF and control mice weighed the same. However, feeding a high fat diet (HFD) elicited a phenotypic difference. HFD-fed FASKOF mice weighed less (Figure 1D)

and had less adiposity as well as more lean tissue compared to controls (Figure 1E). The adiposity effect was seen in both sexes and also in the setting of high carbohydrate/zero fat diet feeding (Table S1). Epididymal fat pads (white adipose tissue, WAT), but not other tissues, from HFD-fed FASKOF mice weighed less than those from control mice (Figure 1F). White adipocytes isolated from FASKOF mice were smaller than adipocytes from control mice with HFD feeding (Figure 1G,H), but there was no effect with chow feeding. Genotype and diet had no effect on adipocyte cell number (not shown), perhaps reflecting induction of adiponectin-Cre expression following adipose tissue development.

The weight of brown adipose tissue (BAT) was not different in mice fed HFD. However, when adult mice were fed a high carbohydrate/zero fat diet, which maximizes effects due to FAS deficiency, the BAT depot in FASKOF mice weighed significantly less than that of control mice (Figure S1A). The histologic appearance of BAT was not different between genotypes in mice fed HFD, but lipid stores were depleted (Figure S1B) and the PPAR $\gamma$  target genes CD36, HSL, and ATGL were decreased (Figure S1C) in the BAT depot from FASKOF mice fed a high carbohydrate/zero fat diet.

Hepatic histologic appearance (Figure S1D) and lipid content (Figure S1E) were not different between control and FASKOF animals.

### Altered Thermogenesis in FASKOF Mice

Food intake was not different between FASKOF and control mice on any diet (Table S1). When studied on a HFD prior to development of statistically significant differences in body weight, FASKOF mice had increased energy expenditure compared to controls (Figure 2A). Systemic glucose tolerance and insulin sensitivity were enhanced in HFD-fed FASKOF mice (notable for less adiposity) compared to controls (Figures 2B,C), but with chow feeding (a condition associated with similar degrees of adiposity in each genotype) there was no difference in glucose tolerance between FASKOF and control mice (Figure S1F). Consistent with the observation that decreased adiposity improves insulin sensitivity in numerous animal models (Elchebly et al., 1999; Masuzaki et al., 2001; Yang et al., 2005; Yuan et al., 2001), levels of phospho-Akt relative to total Akt were increased in skeletal muscle of HFD-fed FASKOF mice (data not shown). Serum leptin was lower (perhaps reflecting decreased adiposity) but adiponectin was unaffected in HFD-fed FASKOF mice (Table S1). Given effects of FAS deletion on other PPAR $\gamma$  genes (see below), it is possible that not all targets of PPAR $\gamma$ , including adiponectin, are affected by FAS deletion. Monitored physical activity was not increased in FASKOF animals (Figure S1G).

Body temperature was not different between control and FASKOF mice at room temperature, there were no apparent brown fat-like adipocytes in the epididymal fat of FASKOF mice, and FASKOF epididymal fat did not have increased expression of the brown fat gene UCP1 (not shown). However, UCP1 expression was strikingly increased in inguinal fat from HFD-fed FASKOF mice as compared to controls (Figure 2D). Expression of PRDM16, a transcriptional coregulator involved in the development of classic BAT as well as brown fat-like adipocytes in subcutaneous white adipose tissue (WAT) (Seale et al., 2011), was also increased as were levels of the brown fat genes Cidea and PGC1 $\alpha$  (Figure 2D). PPAR $\alpha$  is known to induce UCP1 expression (Barbera et al., 2001), and mRNA levels for PPAR $\alpha$  as well as the PPAR $\alpha$ -dependent genes CPT1 and ACO were increased in inguinal fat (Figure 2D). Since PPAR $\alpha$  promotes fatty acid oxidation, we assayed this process in homogenates of WAT as the release of CO<sub>2</sub> from radiolabelled palmitate. In HFD-fed mice, fatty acid oxidation was increased in FASKOF as compared to control mice in inguinal but not epididymal WAT (Figure 2E). To maximize effects due to FAS deficiency, we fed mice a high carbohydrate/zero fat diet and analyzed inguinal fat. Under these conditions, inguinal fat mRNA levels for UCP1, Cidea, and PGC1 $\alpha$  were increased

(Figure S1H). UCP1 protein was increased in inguinal fat from FASKOF as compared to control mice by both Western blotting (Figure 2F) and immunocytochemistry (Figure 2G). With cold exposure, FASKOF mice maintained their body temperature at a significantly higher level than control mice (Figure 2H), suggesting that increased brown fat-like cells in subcutaneous WAT of FASKOF are physiologically relevant.

### FAS Promotes PPAR $\gamma$ Activation and Adipogenesis

PPAR $\gamma$  is necessary and sufficient for adipogenesis (Tontonoz and Spiegelman, 2008) but also mediates HFD-induced hypertrophy of adipocytes (Hosooka et al., 2008; Kubota et al., 1999). Moreover, PPAR $\gamma$  is thought to promote fat development at the expense of myogenesis (Hu et al., 1995; Seale et al., 2008). Previous studies suggested that lipogenic pathways may be required for activating PPAR $\gamma$  by generating its endogenous ligand (Kim and Spiegelman, 1996; Kim et al., 1998) and influencing adipogenesis (Schmid et al., 2005).

Since HFD-fed FASKOF mice have decreased adiposity and reduced adipocyte hypertrophy (Figure 1), we explored the possibility that FAS is involved in PPAR $\gamma$  activation and adipogenesis using mouse embryonic fibroblasts (MEFs) from FAS<sup>lox/lox</sup> animals. Expression of Cre using an adenovirus (Ad-Cre) in these cells decreased FAS protein and impaired adipogenesis (Figure 3A,B). Defective adipogenesis induced by FAS deficiency was rescued by treatment with the PPAR $\gamma$  activator rosiglitazone (Figure 3B, bottom panels), likely due to induction of processes (involving CD36, LPL, and other proteins) that facilitate uptake of lipids from the culture media.

We next transfected HEK 293 cells with cDNAs for PPAR $\gamma$  and a PPAR-dependent luciferase reporter in the presence or absence of FAS knockdown. FAS deficiency decreased luciferase reporter activity, an effect that was rescued with rosiglitazone, suggesting that FAS regulates PPAR $\gamma$  transcriptional activity (Figure 3C). To address possible contributions of ligand-independent effects of FAS knockdown on PPAR $\gamma$  transactivation, we performed luciferase reporter assays using cells transfected with constitutively active PPAR $\gamma$  (VP16-PPAR $\gamma$ ) or wild type PPAR $\gamma$ . FAS knockdown reduced luciferase reporter activity in cells transfected with WT PPAR $\gamma$ , and the effect was significantly greater than in cells transfected with VP16-PPAR $\gamma$  (Figure 3D). Knockdown of FAS in primary MEFs decreased expression of the PPAR $\gamma$  target genes aP2 and CD36 but increased expression of the early myogenesis markers MyoD and myogenin, effects that were reversed with rosiglitazone (Figure 3E). Consistent with induction of myogenic markers, FAS inactivation was associated with myotube formation under pro-myogenic culture conditions (Figure 3F). FAS knockdown decreased levels of proteins regulated by PPAR $\gamma$  in 3T3-L1 adipocytes (Figure 3G). PPAR $\gamma$  target gene expression was restored in these murine cells with FAS knockdown by expressing human FAS (Figure 3H). PPAR $\gamma$  target genes were also decreased in the adipose tissue of FASKOF mice (Figure 3I). To determine if FAS deficiency is affecting PPAR $\gamma$  expression as opposed to its transcriptional activity, we fed mice a high carbohydrate/zero fat diet to maximize effects due to FAS deficiency and subjected gonadal WAT to Western blotting. There was no effect on PPAR $\gamma$  protein mass while protein levels of the PPAR $\gamma$  target aP2 were decreased in FASKOF as compared to control mice (Figure 3J). One plausible interpretation of these results is that FAS is part of a lipogenic pathway that regulates adipogenesis at the expense of myogenesis by generating endogenous ligands for PPAR $\gamma$  that promote its transcriptional activity.

### Identification of FAS-Dependent Diacyl and Alkyl Ether Lipid Species Bound to PPAR $\gamma$

There are probably numerous PPAR $\gamma$  endogenous ligands that may be generated under conditions requiring alterations in adipocyte function, but ligands are initially produced early during adipocyte differentiation (Tzameli et al., 2004). To isolate such putative FAS-

dependent ligands, we used mass spectrometry after infecting MEFs with an adenovirus encoding FLAG-tagged PPAR $\gamma$  and inducing differentiation (Figure 4A). PPAR $\gamma$  was isolated by affinity from cells in the presence or absence of FAS knockdown (Figure 4B) and associated lipids were analyzed by mass spectrometry (Figure 4C). We identified several phosphatidylcholine species with diacyl (ester bond-linked) or 1-*O*-alkyl (ether bond-linked) side chains associated with PPAR $\gamma$  that were competitively displaced by rosiglitazone (not shown). Alkyl ether lipids were particularly enriched in PPAR $\gamma$  samples compared to controls (Table S2). The species at  $m/z$  752 [M+Li]<sup>+</sup> was most frequently associated with PPAR $\gamma$  and tandem mass spectrometry identified it as 1-*O*-octadecenyl-2-palmitoyl-3-glycerophosphocholine (18:1e/16:0-GPC) (Figure S2). We synthesized this alkyl ether lipid and used it to treat cultured cells. 18:1e/16:0-GPC increased PPAR $\gamma$ -dependent luciferase reporter activity in a dose-dependent fashion (Figure 4D) but was less potent than rosiglitazone. 20  $\mu$ M 18:1e/16:0-GPC significantly increased the expression of PPAR $\gamma$  target genes in differentiating 3T3-L1 adipocytes (Figure 4E).

In order to provide insight into the interaction between 18:1e/16:0-GPC and the PPAR $\gamma$  ligand binding domain (LBD), we developed a GST-pulldown assay of PPAR $\gamma$  ligand binding based on the ligand-dependent interaction between an N-terminal region of CBP1 and the PPAR $\gamma$  LBD (Gelman et al., 1999). 18:1e/16:0-GPC increased the interaction between the GST-tagged PPAR $\gamma$  LBD and the myc-tagged CBP1 N-terminus in a dose-dependent manner (Figure S3A). However, 18:1e/16:0-GPC did not increase the interaction between the GST-tagged LBD of a different nuclear receptor, PPAR $\alpha$ , and the myc-tagged CBP1 N-terminus (Figure S3B). To provide additional evidence that this ether lipid enhances PPAR $\gamma$  transcription due to agonism, we added 18:1e/16:0-GPC to terminally differentiated 3T3-L1 adipocytes. Both 18:1e/16:0-GPC and rosiglitazone increased LPL gene expression in differentiated adipocytes that were treated with a control shRNA prior to induction of differentiation (Figure S3C). In cells prevented from differentiating into adipocytes by FAS knockdown, treatment with either 18:1e/16:0-GPC or rosiglitazone after completion of the differentiation protocol (with dexamethasone, IBMX, and insulin followed by additional insulin treatment) did not restore full LPL expression (Figure S3C). FAS deficiency decreased expression of PPAR $\gamma$ -dependent genes (Figure 3I) while increasing expression of PPAR $\alpha$ -dependent genes (Figure 2D). When FAS expression was knocked down in 3T3-L1 cells that were subsequently induced to differentiate into adipocytes, the FAS-deficiency-associated increase in ACO gene expression was significantly decreased when cells were differentiated in the presence of the selective PPAR $\alpha$  antagonist GW6471 (Figure S3D). These results suggest that an FAS-dependent ether lipid interacts with PPAR $\gamma$  but not PPAR $\alpha$  and that FAS deficiency is associated with decreased activation of PPAR $\gamma$  and increased activation of PPAR $\alpha$ .

### Cloning and Characterization of PexRAP

Ether lipid synthesis in mammals occurs through the peroxisomal acyl dihydroxyacetone phosphate (DHAP) pathway, allowing synthesis of lysophosphatidic acid as an alternative to direct acylation of glycerol 3-phosphate. This pathway is obligatory for synthesis of ether lipids including platelet activating factors and plasmalogens (Hajra and Das, 1996; Hajra et al., 2000; McIntyre et al., 2008) (Figure 5A). The terminal enzyme activity in this pathway, acyl/alkyl DHAP reductase, was purified and characterized from guinea pig liver (LaBelle and Hajra, 1974), but the gene encoding this protein has not been identified in mammals (McIntyre et al., 2008). Since a yeast enzyme (Ayr1p) (Athenstaedt and Daum, 2000) that catalyzes this reaction has been cloned and characterized, we used this sequence to identify DHRS7b, a protein of unknown function, as a mammalian ortholog (Figure 5B). We renamed this protein PexRAP, for Peroxisomal Reductase Activating PPAR $\gamma$ . Gradient fractionation of 3T3-L1 adipocytes showed that PexRAP is enriched in fractions containing

peroxisomal markers, such as PMP70 and catalase (Figure 5C). Myc-tagged PexRAP co-immunoprecipitated with Pex19 (peroxisomal biogenesis factor 19, an import receptor for peroxisomal membrane proteins) (Figure 5D), and this interaction was confirmed in pulldown experiments using GST-PexRAP (Figure 5E).

To demonstrate that PexRAP mediates its predicted enzyme activity, we knocked down PexRAP expression in MEFs (Figure 5F) and found decreased levels of 1-*O*-alkyl ether phospholipids as well as certain diacyl phospholipids (Figure 5G), some of which also arise from the DHAP pathway. 18:1e/16:0-GPC was detected in these experiments as  $m/z$  746 [M+H]<sup>+</sup> since these experiments were performed with protonated species; 18:1e/16:0-GPC was detected as  $m/z$  752 using lithiated species in Figure 4C. PexRAP protein was detected in multiple tissues, but levels were low in skeletal muscle (Figure 5H). The overall expression of PexRAP in BAT was relatively low and BAT primarily expressed a shorter isoform (which lacks 9 amino acid residues at the N-terminus), suggesting that PexRAP may have a different role in BAT compared to WAT. Both PexRAP and FAS proteins markedly increase early during differentiation of 3T3-L1 adipocytes, prior to similar increases in proteins such as C/EBP $\alpha$  and aP2 known to be induced by PPAR $\gamma$  activation (Figure 5I). Thus, PexRAP is peroxisomal, its inactivation decreases lipids associated with PPAR $\gamma$ , and its temporal relationship during differentiation with other adipocyte proteins suggests that it could be involved in adipogenesis.

### PexRAP is Required for Adipogenesis

To address the role of PexRAP in adipogenesis, we knocked down its expression in 3T3-L1 cells. Adipogenesis (assessed by both Nile red staining and triglyceride content) was abrogated with PexRAP knockdown and rescued with rosiglitazone (Figures 6A,B), suggesting that PexRAP, like FAS (Figure 3B), affects PPAR $\gamma$  activation. Knockdown of PexRAP or DHAP acyltransferase (DHAPAT, the enzyme immediately upstream of PexRAP, Figure 5A) in 3T3-L1 adipocytes decreased expression of PPAR $\gamma$  target genes (Figure 6C). Rosiglitazone treatment rescued the effect of PexRAP or DHAPAT knockdown on PPAR $\gamma$  target genes (Figure 6D).

### PexRAP Knockdown in Mice Alters Body Composition and Metabolism

We translated these observations to HFD-fed C57BL/6J mice, characterized by increased adiposity and insulin resistance. A series of PexRAP antisense oligonucleotides (ASOs) were screened for effectiveness (not shown) and results of PexRAP knockdown for two of the most promising are shown in Figure 7A using Hepa1-6 cells. ASO2 was selected for use in mice. Intraperitoneal administration of ASO2 at up to 20 mg/kg twice a week for three weeks resulted in a dose-dependent decrease in PexRAP protein in WAT and liver (but not in brain or skeletal muscle, Figures 7B, S4A). Mice were fed a HFD for four weeks to increase adiposity and then animals were injected twice a week with 20 mg/kg of ASO2 or the control ASO for 24 days while HFD was continued. ASO treatment had no effect on liver function tests or liver histology (not shown). Liver fat content was nearly significantly lower ( $P=0.072$ ) with ASO treatment. Food intake was unaffected (Table S3). However, this intervention decreased expression of PexRAP as well as PPAR $\gamma$  target genes (including PPAR $\gamma$  itself) in WAT (Figure 7C). PexRAP knockdown in HFD-fed mice also decreased adiposity, increased leanness, and decreased fasting glucose (Figure 7D, Table S3). Glucose tolerance was improved and insulin levels were lower in HFD-fed mice treated with the PexRAP ASO (Figure 7E,F).

## DISCUSSION

These studies suggest that depletion of FAS in adipose tissue suppresses HFD-induced obesity. FAS is a minor contributor to cellular lipid stores with high fat feeding (Aarsland et al., 1996; Letexier et al., 2003; McDevitt et al., 2001); HFD feeding decreases FAS expression (Coupe et al., 1990; Kersten, 2001). Thus, it is unlikely that the reduced adiposity observed in the HFD-fed FASKOF mice was due to the inability to synthesize fatty acids *per se*. Rather, our results suggest that inhibiting a lipogenic pathway initiated by FAS increases thermogenesis and reduces activation of PPAR $\gamma$ . Increased energy expenditure comes not from effects on classic BAT but instead by inducing the formation of brown fat-like (“brite”) cells in subcutaneous adipose tissue (Seale et al., 2011).

In addition to inducing brown fat-like cells in subcutaneous fat, FAS deletion decreased PPAR $\gamma$  transcriptional activity. It is possible that these transcriptional effects are unrelated or only partially related to the phenotype of resistance to diet-induced obesity caused by increased brite cells. PPAR $\gamma$  agonism can induce UCP1 gene expression and produce small adipocytes in WAT (de Souza et al., 2001; Fukui et al., 2000; Tiraby et al., 2003), similar to the FASKOF mouse phenotype, and yet FASKOF mice have decreased PPAR $\gamma$  activation. However, pharmacologic agonism of PPAR $\gamma$  promotes adiposity, while FASKOF mice have less adiposity. Effects on PPAR $\alpha$  with FAS deletion could provide a plausible explanation. PPAR $\alpha$  and its targets are induced in FASKOF adipose tissue (Figure 2D). PPAR $\alpha$  inhibition decreases induction of the PPAR $\alpha$  target gene ACO with FAS knockdown in 3T3-L1 cells (Figure S3D). PPAR $\alpha$  agonism can also induce UCP1 gene expression (Barbera et al., 2001) as well as decrease adipocyte size (Tsuchida et al., 2005), and the acute effects of PPAR $\alpha$  activation on UCP1 gene expression may exceed those of PPAR $\gamma$  (Pedraza et al., 2001). Decreased PPAR $\gamma$  transcriptional activity could reflect the lack of an FAS-associated lipid ligand, allowing increased PPAR $\alpha$  activity and induction of UCP1. In support of this notion, induction of UCP1 and the development of brown fat-like cells by FNDC5 (cleaved to form irisin) occurs in part through PPAR $\alpha$  (Bostrom et al., 2012).

Our data point to a pathway (Figure 7G, left) in which lipids synthesized by FAS serve as substrate for PexRAP, which generates alkyl ether lipids that are potential endogenous PPAR $\gamma$  ligands. Disruption of FAS (Figure 7G, right) decreases these ether lipids, altering the coactivator milieu to favor PPAR $\alpha$ -dependent gene expression.

Several lines of evidence support the concept that a lipogenic pathway localized to peroxisomes is important for endogenous activation of PPAR $\gamma$ . The PPAR family was named because of the ability to be activated by agents that increase the number of peroxisomes (Dreyer et al., 1992; Issemann and Green, 1990). The number of peroxisomes is dramatically increased during differentiation of 3T3-L1 adipocytes (Novikoff and Novikoff, 1982; Novikoff et al., 1980), a PPAR $\gamma$ -dependent process. Consistent with our observation that PexRAP expression is induced during adipogenesis, previous studies suggest that the activities of various enzymes in the peroxisomal ether lipid synthetic pathway increase during differentiation of 3T3-L1 adipocytes (Hajra et al., 2000).

There is precedent for PPAR $\gamma$  activation by alkyl ether lipids. Azelaoyl PAF (1-*O*-hexadecyl-2-*O*-(9-carboxyoctanoyl)-sn-glycerol-3-phosphocholine), reported to be equipotent to rosiglitazone (Davies et al., 2001), and 1-*O*-alkyl glycerol 3-phosphate (McIntyre et al., 2003; Tsukahara et al., 2006), synthesized directly by PexRAP (see Figure 5A), are thought to be PPAR $\gamma$  ligands. Because PPAR $\gamma$  has a capacious ligand binding pocket (Schupp and Lazar, 2010), it is possible that instead of a single authentic endogenous

ligand, multiple lipids are recruited to the receptor depending on the physiological context, with variable effects on transcriptional activity (Lodhi et al., 2011; Schupp and Lazar, 2010).

ASO-mediated inhibition of PexRAP decreased adiposity and improved glucose metabolism, probably by activating thermogenesis in subcutaneous WAT. In studies to be reported elsewhere, we have observed that PexRAP deficiency in adipose tissue achieved by crossing adiponectin-Cre mice with floxed PexRAP animals robustly induces UCP1 expression in subcutaneous but not epididymal WAT.

Adipose-specific knockout of PPAR $\gamma$  in mice has yielded conflicting results: one group reported lipodystrophy and insulin resistance (He et al., 2003) while another found enhanced insulin sensitivity (Jones et al., 2005). Certain human PPAR $\gamma$  mutations cause lipodystrophy and insulin resistance, likely through a dominant-negative effect to disrupt interaction with coactivators (Agostini et al., 2006). In our studies, neither ASO-mediated PexRAP knockdown in mice nor Cre-mediated adipose-specific FAS knockout in mice produced lipodystrophy. Both decreased adiposity and improved glucose metabolism. PPAR $\gamma$  haploinsufficiency in mice (Kubota et al., 1999; Miles et al., 2000) also decreases adiposity and increases insulin sensitivity, but this genetic effect is not limited to adipose tissue. A Pro12Ala PPAR $\gamma$  mutation in mice (Heikkinen et al., 2009) and humans (Huguenin and Rosa, 2010) decreases (but does not abolish) PPAR $\gamma$  transcriptional activity and results in decreased adiposity and increased insulin sensitivity, although this mutation is not adipose-specific.

Inhibiting FAS or the peroxisomal enzyme PexRAP in adipose tissue alters body composition and improves glucose metabolism in the setting of a high fat diet. Both represent attractive targets for novel diabetes and obesity therapies.

## EXPERIMENTAL PROCEDURES

### Animals

Mice with a floxed FAS locus (FAS<sup>lox/lox</sup>) (Chakravarthy et al., 2005) were crossed with transgenic mice (a gift from Evan Rosen, BI Deaconess) expressing Cre recombinase under the control of the adiponectin promoter (Eguchi et al., 2011) to obtain FASKOF mice that were studied after backcrossing 7 times with pure C57BL/6J mice. Genotyping was performed using previously described primer sets and diets included Purina 4043 control chow, Harlan Teklad TD 88137 high fat diet, and Harlan Teklad TD03314 high carbohydrate/zero fat diet. Unless indicated otherwise, male FASKOF mice and control littermates at 8–12 weeks of age were used for experiments. For antisense oligonucleotide studies, 8 week-old C57BL/6J mice were used. All protocols were approved by the Washington University Animal Studies Committee.

### Cell Culture

Primary mouse embryonic fibroblasts (MEFs) were isolated at 13.5 days post conception from FAS<sup>lox/lox</sup> embryos as previously described (Razani et al., 2001) and maintained in DMEM+10% FBS. MEFs were differentiated to adipocytes by treatment with 1  $\mu$ M dexamethasone, 5  $\mu$ g/ml insulin and 0.5 mM IBMX for 14 days, followed by supplemental 5  $\mu$ g/ml insulin alone for an additional 4 days. 3T3-L1 cells were maintained in DMEM +10% NCS and differentiated to adipocytes as previously described (Lodhi et al., 2007). CV-1, HEK 293 and HEK 293T cells were maintained in DMEM+10% FBS.



### Lentiviral shRNA-mediated Knockdown

Plasmids encoding shRNA for mouse FAS (TRCN0000075703), PexRAP (TRCN0000181732 and 0000198546) and DHAPAT (TRCN0000193539) were obtained from Open Biosystems (Huntsville, AL). Packaging vector psPAX2 (12260), envelope vector pMD2.G (12259) and scrambled shRNA plasmid (1864) were obtained from Addgene. 293T cells in 10 cm dishes were transfected using Fugene 6 with 2.66  $\mu$ g psPAX2, 0.75  $\mu$ g pMD2.G, and 3  $\mu$ g shRNA plasmid. After 48 h, media were collected, filtered using 0.45  $\mu$ m syringe filters, and used to treat cells. After 36 h, cells were selected with puromycin and knockdown was assessed after an additional 48 h.

### Identification of Alkyl Ether GPC Lipids Associated with PPAR $\gamma$

The strategy for detecting endogenous lipids associated with PPAR $\gamma$  involved adenovirus-mediated expression of FLAG-tagged PPAR $\gamma$  or GFP (as control) in cells induced to differentiate into adipocytes. Nuclear fractions, prepared from cell lysates and subjected to hypotonic lysis as described (Chakravarthy et al., 2009), were incubated with an antibody recognizing the FLAG epitope to capture the PPAR $\gamma$  construct and any associated lipids under conditions (no detergent or high salt elution buffers) unlikely to disrupt potential ligand/nuclear factor interaction.

Affinity matrix eluates (with equal protein content) of nuclear fractions from cells treated with Ad-GFP (as a control) or Ad-PPAR $\gamma$  were subjected to lipid extraction. These extracts were mixed with an internal standard [(14:0/14:0)-GPC] and analyzed as [M+Li]<sup>+</sup>, [M+H]<sup>+</sup>, or [M+Na]<sup>+</sup> ions by positive ion ESI/MS or as [M+CH<sub>3</sub>CO<sub>2</sub>]<sup>-</sup> ions by negative ion ESI/MS (Hsu and Turk, 2007; Hsu et al., 2003). To determine the identity of the lithiated lipid species of *m/z* 752, we performed multigenerational tandem MS on a linear ion trap instrument. Collisionally-activated dissociation (CAD) was employed to deduce structures of R<sub>1</sub> and R<sub>2</sub> substituents. Additional details are provided in Figure S3.

### GST-PexRAP Pull-down Assays

3T3-L1 adipocytes were lysed using a buffer containing 50 mM HEPES (pH 7.4), 4 mM EDTA, 2 mM EGTA, 2 mM sodium pyrophosphate, 1% Triton X-100, 10 mM NaF, and protease inhibitors. Lysates were mixed with an equal volume of the same buffer lacking Triton X-100, then 5  $\mu$ g of GST or GST-PexRAP was added and samples were rocked at 4°C. After 2 h, samples were centrifuged at 2500  $\times$  g for 1 min, beads were washed 5 times with 1 ml of the lysis buffer containing Triton X-100, then 2 $\times$  SDS-PAGE sample buffer was added and samples were subjected to SDS-PAGE.

### Antisense Oligonucleotides

ASOs were synthesized by TriLink Biotechnologies (San Diego, CA). The first 5 and last 5 nucleotides were substituted with 2' *O*-methyl RNA bases; all of the bases had phosphorothioate linkages. The PexRAP ASO (RNA bases underlined) is: 5' GGUUGGTGTGTCTGTCCCUG 3'. The control oligonucleotide is: 5' CCUCCCTGAAGGTTCCUCC 3'. Both were purified by anion exchange HPLC, lyophilized, reconstituted with 0.9% normal saline, and then injected intraperitoneally.

### Statistical Analysis

Data are expressed as mean  $\pm$  SEM. Comparisons between two groups were performed using an unpaired, two-tailed t-test. ANOVA was used for more than two groups and post-testing was performed using Tukey's post test.

## Supplementary Material

Refer to Web version on PubMed Central for supplementary material.

## Acknowledgments

This work was supported by NIH grants DK088083, DK076729, F32 DK083895, KO8 HL098559, DK20579, DK56341, DK34388, RR00954, and T32 DK07120. Alan Bohrer provided mass spectrometry expertise.

## REFERENCES

- Aarsland A, Chinkes D, Wolfe RR. Contributions of de novo synthesis of fatty acids to total VLDL-triglyceride secretion during prolonged hyperglycemia/hyperinsulinemia in normal man. *J Clin Invest.* 1996; 98:2008–2017. [PubMed: 8903319]
- Agostini M, Schoenmakers E, Mitchell C, Szatmari I, Savage D, Smith A, Rajanayagam O, Semple R, Luan J, Bath L, et al. Non-DNA binding, dominant-negative, human PPARgamma mutations cause lipodystrophic insulin resistance. *Cell Metab.* 2006; 4:303–311. [PubMed: 17011503]
- Athenstaedt K, Daum G. 1-Acylidihydroxyacetone-phosphate reductase (Ayr1p) of the yeast *Saccharomyces cerevisiae* encoded by the open reading frame YIL124w is a major component of lipid particles. *J Biol Chem.* 2000; 275:235–240. [PubMed: 10617610]
- Barbera MJ, Schluter A, Pedraza N, Iglesias R, Villarroya F, Giralt M. Peroxisome proliferator-activated receptor alpha activates transcription of the brown fat uncoupling protein-1 gene. A link between regulation of the thermogenic and lipid oxidation pathways in the brown fat cell. *J Biol Chem.* 2001; 276:1486–1493. [PubMed: 11050084]
- Bostrom P, Wu J, Jedrychowski MP, Korde A, Ye L, Lo JC, Rasbach KA, Bostrom EA, Choi JH, Long JZ, et al. A PGC1-alpha-dependent myokine that drives brown-fat-like development of white fat and thermogenesis. *Nature.* 2012; 481:463–468. [PubMed: 22237023]
- Chakravarthy MV, Lodhi IJ, Yin L, Malapaka RR, Xu HE, Turk J, Semenkovich CF. Identification of a physiologically relevant endogenous ligand for PPARalpha in liver. *Cell.* 2009; 138:476–488. [PubMed: 19646743]
- Chakravarthy MV, Pan Z, Zhu Y, Tordjman K, Schneider JG, Coleman T, Turk J, Semenkovich CF. “New” hepatic fat activates PPARalpha to maintain glucose, lipid, and cholesterol homeostasis. *Cell Metab.* 2005; 1:309–322. [PubMed: 16054078]
- Coupe C, Perdreau D, Ferre P, Hitier Y, Narkewicz M, Girard J. Lipogenic enzyme activities and mRNA in rat adipose tissue at weaning. *Am J Physiol.* 1990; 258:E126–133. [PubMed: 1967906]
- Davies SS, Pontsler AV, Marathe GK, Harrison KA, Murphy RC, Hinshaw JC, Prestwich GD, Hilaire AS, Prescott SM, Zimmerman GA, et al. Oxidized alkyl phospholipids are specific, high affinity peroxisome proliferator-activated receptor gamma ligands and agonists. *J Biol Chem.* 2001; 276:16015–16023. [PubMed: 11279149]
- de Souza CJ, Eckhardt M, Gagen K, Dong M, Chen W, Laurent D, Burkey BF. Effects of pioglitazone on adipose tissue remodeling within the setting of obesity and insulin resistance. *Diabetes.* 2001; 50:1863–1871. [PubMed: 11473050]
- Dreyer C, Krey G, Keller H, Givel F, Helftenbein G, Wahli W. Control of the peroxisomal beta-oxidation pathway by a novel family of nuclear hormone receptors. *Cell.* 1992; 68:879–887. [PubMed: 1312391]
- Eguchi J, Wang X, Yu S, Kershaw EE, Chiu PC, Dushay J, Estall JL, Klein U, Maratos-Flier E, Rosen ED. Transcriptional control of adipose lipid handling by IRF4. *Cell Metab.* 2011; 13:249–259. [PubMed: 21356515]
- Elchebly M, Payette P, Michaliszyn E, Cromlish W, Collins S, Loy AL, Normandin D, Cheng A, Himms-Hagen J, Chan CC, et al. Increased insulin sensitivity and obesity resistance in mice lacking the protein tyrosine phosphatase-1B gene. *Science.* 1999; 283:1544–1548. [PubMed: 10066179]
- Finucane MM, Stevens GA, Cowan MJ, Danaei G, Lin JK, Paciorek CJ, Singh GM, Gutierrez HR, Lu Y, Bahalim AN, et al. National, regional, and global trends in body-mass index since 1980:

- systematic analysis of health examination surveys and epidemiological studies with 960 country-years and 9.1 million participants. *Lancet*. 2011; 377:557–567. [PubMed: 21295846]
- Fukui Y, Masui S, Osada S, Umesono K, Motojima K. A new thiazolidinedione, NC-2100, which is a weak PPAR-gamma activator, exhibits potent antidiabetic effects and induces uncoupling protein 1 in white adipose tissue of KKAy obese mice. *Diabetes*. 2000; 49:759–767. [PubMed: 10905484]
- Gelman L, Zhou G, Fajas L, Raspe E, Fruchart JC, Auwerx J. p300 interacts with the N- and C-terminal part of PPARgamma2 in a ligand-independent and -dependent manner, respectively. *J Biol Chem*. 1999; 274:7681–7688. [PubMed: 10075656]
- Hajra AK, Das AK. Lipid biosynthesis in peroxisomes. *Ann N Y Acad Sci*. 1996; 804:129–141. [PubMed: 8993541]
- Hajra AK, Larkins LK, Das AK, Hemati N, Erickson RL, MacDougald OA. Induction of the peroxisomal glycerolipid-synthesizing enzymes during differentiation of 3T3-L1 adipocytes. Role in triacylglycerol synthesis. *J Biol Chem*. 2000; 275:9441–9446. [PubMed: 10734090]
- He W, Barak Y, Hevener A, Olson P, Liao D, Le J, Nelson M, Ong E, Olefsky JM, Evans RM. Adipose-specific peroxisome proliferator-activated receptor gamma knockout causes insulin resistance in fat and liver but not in muscle. *Proc Natl Acad Sci U S A*. 2003; 100:15712–15717. [PubMed: 14660788]
- Heikkinen S, Argmann C, Feige JN, Koutnikova H, Champy MF, Dali-Youcef N, Schadt EE, Laakso M, Auwerx J. The Pro12Ala PPARgamma2 variant determines metabolism at the gene-environment interface. *Cell Metab*. 2009; 9:88–98. [PubMed: 19117549]
- Hosooka T, Noguchi T, Kotani K, Nakamura T, Sakaue H, Inoue H, Ogawa W, Tobimatsu K, Takazawa K, Sakai M, et al. Dok1 mediates high-fat diet-induced adipocyte hypertrophy and obesity through modulation of PPAR-gamma phosphorylation. *Nat Med*. 2008; 14:188–193. [PubMed: 18204460]
- Hsu FF, Turk J. Differentiation of 1-O-alk-1'-enyl-2-acyl and 1-O-alkyl-2-acyl glycerophospholipids by multiple-stage linear ion-trap mass spectrometry with electrospray ionization. *J Am Soc Mass Spectrom*. 2007; 18:2065–2073. [PubMed: 17913512]
- Hsu FF, Turk J, Thukkani AK, Messner MC, Wildsmith KR, Ford DA. Characterization of alkylacyl, alk-1-enylacyl and lyso subclasses of glycerophosphocholine by tandem quadrupole mass spectrometry with electrospray ionization. *J Mass Spectrom*. 2003; 38:752–763. [PubMed: 12898655]
- Hu E, Tontonoz P, Spiegelman BM. Transdifferentiation of myoblasts by the adipogenic transcription factors PPAR gamma and C/EBP alpha. *Proc Natl Acad Sci U S A*. 1995; 92:9856–9860. [PubMed: 7568232]
- Huguenin GV, Rosa G. The Ala allele in the PPAR-gamma2 gene is associated with reduced risk of type 2 diabetes mellitus in Caucasians and improved insulin sensitivity in overweight subjects. *Br J Nutr*. 2010; 104:488–497. [PubMed: 20420754]
- Issemann I, Green S. Activation of a member of the steroid hormone receptor superfamily by peroxisome proliferators. *Nature*. 1990; 347:645–650. [PubMed: 2129546]
- Jones JR, Barrick C, Kim KA, Lindner J, Blondeau B, Fujimoto Y, Shiota M, Kesterson RA, Kahn BB, Magnuson MA. Deletion of PPARgamma in adipose tissues of mice protects against high fat diet-induced obesity and insulin resistance. *Proc Natl Acad Sci U S A*. 2005; 102:6207–6212. [PubMed: 15833818]
- Kersten S. Mechanisms of nutritional and hormonal regulation of lipogenesis. *EMBO Rep*. 2001; 2:282–286. [PubMed: 11306547]
- Kim JB, Spiegelman BM. ADD1/SREBP1 promotes adipocyte differentiation and gene expression linked to fatty acid metabolism. *Genes Dev*. 1996; 10:1096–1107. [PubMed: 8654925]
- Kim JB, Wright HM, Wright M, Spiegelman BM. ADD1/SREBP1 activates PPARgamma through the production of endogenous ligand. *Proc Natl Acad Sci U S A*. 1998; 95:4333–4337. [PubMed: 9539737]
- Kubota N, Terauchi Y, Miki H, Tamemoto H, Yamauchi T, Komeda K, Satoh S, Nakano R, Ishii C, Sugiyama T, et al. PPAR gamma mediates high-fat diet-induced adipocyte hypertrophy and insulin resistance. *Mol Cell*. 1999; 4:597–609. [PubMed: 10549291]

- LaBelle EF Jr, Hajra AK. Purification and kinetic properties of acyl and alkyl dihydroxyacetone phosphate oxidoreductase. *J Biol Chem.* 1974; 249:6936–6944. [PubMed: 4153765]
- Letexier D, Pinteur C, Large V, Frering V, Beylot M. Comparison of the expression and activity of the lipogenic pathway in human and rat adipose tissue. *J Lipid Res.* 2003; 44:2127–2134. [PubMed: 12897191]
- Lodhi IJ, Chiang SH, Chang L, Vollenweider D, Watson RT, Inoue M, Pessin JE, Saltiel AR. Gapex-5, a Rab31 guanine nucleotide exchange factor that regulates Glut4 trafficking in adipocytes. *Cell Metab.* 2007; 5:59–72. [PubMed: 17189207]
- Lodhi IJ, Wei X, Semenkovich CF. Lipoexpediency: de novo lipogenesis as a metabolic signal transmitter. *Trends Endocrinol Metab.* 2011; 22:1–8. [PubMed: 20889351]
- Lu M, Sarruf DA, Talukdar S, Sharma S, Li P, Bandyopadhyay G, Nalbandian S, Fan W, Gayen JR, Mahata SK, et al. Brain PPAR-gamma promotes obesity and is required for the insulin-sensitizing effect of thiazolidinediones. *Nat Med.* 2011; 17:618–622. [PubMed: 21532596]
- Masuzaki H, Paterson J, Shinyama H, Morton NM, Mullins JJ, Seckl JR, Flier JS. A transgenic model of visceral obesity and the metabolic syndrome. *Science.* 2001; 294:2166–2170. [PubMed: 11739957]
- McDevitt RM, Bott SJ, Harding M, Coward WA, Bluck LJ, Prentice AM. De novo lipogenesis during controlled overfeeding with sucrose or glucose in lean and obese women. *Am J Clin Nutr.* 2001; 74:737–746. [PubMed: 11722954]
- McIntyre TM, Pontsler AV, Silva AR, St Hilaire A, Xu Y, Hinshaw JC, Zimmerman GA, Hama K, Aoki J, Arai H, et al. Identification of an intracellular receptor for lysophosphatidic acid (LPA): LPA is a transcellular PPARgamma agonist. *Proc Natl Acad Sci U S A.* 2003; 100:131–136. [PubMed: 12502787]
- McIntyre, TM.; Snyder, F.; Marathe, GK. Ether-linked lipids and their bioactive species In *Biochemistry of lipids, lipoproteins and membranes.* Vance, DE.; Vance, JE., editors. Elsevier; Amsterdam; Boston: 2008. p. 245-276.
- Miles PD, Barak Y, He W, Evans RM, Olefsky JM. Improved insulin-sensitivity in mice heterozygous for PPAR-gamma deficiency. *J Clin Invest.* 2000; 105:287–292. [PubMed: 10675354]
- Moreno-Navarrete JM, Botas P, Valdes S, Ortega FJ, Delgado E, Vazquez-Martin A, Bassols J, Pardo G, Ricart W, Menendez JA, et al. Val1483Ile in FASN gene is linked to central obesity and insulin sensitivity in adult white men. *Obesity (Silver Spring).* 2009; 17:1755–1761. [PubMed: 19300427]
- Novikoff AB, Novikoff PM. Microperoxisomes and peroxisomes in relation to lipid metabolism. *Ann N Y Acad Sci.* 1982; 386:138–152. [PubMed: 6953844]
- Novikoff AB, Novikoff PM, Rosen OM, Rubin CS. Organelle relationships in cultured 3T3-L1 preadipocytes. *J Cell Biol.* 1980; 87:180–196. [PubMed: 7191426]
- Pedraza N, Solanes G, Iglesias R, Vazquez M, Giralt M, Villarroya F. Differential regulation of expression of genes encoding uncoupling proteins 2 and 3 in brown adipose tissue during lactation in mice. *Biochem J.* 2001; 355:105–111. [PubMed: 11256954]
- Postic C, Girard J. Contribution of de novo fatty acid synthesis to hepatic steatosis and insulin resistance: lessons from genetically engineered mice. *J Clin Invest.* 2008; 118:829–838. [PubMed: 18317565]
- Razani B, Engelman JA, Wang XB, Schubert W, Zhang XL, Marks CB, Macaluso F, Russell RG, Li M, Pestell RG, et al. Caveolin-1 null mice are viable but show evidence of hyperproliferative and vascular abnormalities. *J Biol Chem.* 2001; 276:38121–38138. [PubMed: 11457855]
- Roberts R, Hodson L, Dennis AL, Neville MJ, Humphreys SM, Harnden KE, Micklem KJ, Frayn KN. Markers of de novo lipogenesis in adipose tissue: associations with small adipocytes and insulin sensitivity in humans. *Diabetologia.* 2009; 52:882–890. [PubMed: 19252892]
- Ryan KK, Li B, Grayson BE, Matter EK, Woods SC, Seeley RJ. A role for central nervous system PPAR-gamma in the regulation of energy balance. *Nat Med.* 2011; 17:623–626. [PubMed: 21532595]
- Schleinitz D, Kloting N, Korner A, Berndt J, Reichenbacher M, Tonjes A, Ruschke K, Bottcher Y, Dietrich K, Enigk B, et al. Effect of genetic variation in the human fatty acid synthase gene (FASN) on obesity and fat depot-specific mRNA expression. *Obesity (Silver Spring).* 2011; 18:1218–1225. [PubMed: 19876008]

- Schmid B, Rippmann JF, Tadayyon M, Hamilton BS. Inhibition of fatty acid synthase prevents preadipocyte differentiation. *Biochem Biophys Res Commun.* 2005; 328:1073–1082. [PubMed: 15707987]
- Schupp M, Lazar MA. Endogenous ligands for nuclear receptors: digging deeper. *J Biol Chem.* 2010; 285:40409–40415. [PubMed: 20956526]
- Seale P, Bjork B, Yang W, Kajimura S, Chin S, Kuang S, Scime A, Devarakonda S, Conroe HM, Erdjument-Bromage H, et al. PRDM16 controls a brown fat/skeletal muscle switch. *Nature.* 2008; 454:961–967. [PubMed: 18719582]
- Seale P, Conroe HM, Estall J, Kajimura S, Frontini A, Ishibashi J, Cohen P, Cinti S, Spiegelman BM. Prdm16 determines the thermogenic program of subcutaneous white adipose tissue in mice. *J Clin Invest.* 2011; 121:96–105. [PubMed: 21123942]
- Semenkovich CF. Regulation of fatty acid synthase (FAS). *Prog Lipid Res.* 1997; 36:43–53. [PubMed: 9373620]
- Seshasai SR, Kaptoge S, Thompson A, Di Angelantonio E, Gao P, Sarwar N, Whincup PH, Mukamal KJ, Gillum RF, Holme I, et al. Diabetes mellitus, fasting glucose, and risk of cause-specific death. *N Engl J Med.* 2011; 364:829–841. [PubMed: 21366474]
- Tiraby C, Tavernier G, Lefort C, Larrouy D, Bouillaud F, Ricquier D, Langin D. Acquisition of brown fat cell features by human white adipocytes. *J Biol Chem.* 2003; 278:33370–33376. [PubMed: 12807871]
- Tontonoz P, Spiegelman BM. Fat and beyond: the diverse biology of PPARgamma. *Annu Rev Biochem.* 2008; 77:289–312. [PubMed: 18518822]
- Tsuchida A, Yamauchi T, Takekawa S, Hada Y, Ito Y, Maki T, Kadowaki T. Peroxisome proliferator-activated receptor (PPAR)alpha activation increases adiponectin receptors and reduces obesity-related inflammation in adipose tissue: comparison of activation of PPARalpha, PPARgamma, and their combination. *Diabetes.* 2005; 54:3358–3370. [PubMed: 16306350]
- Tsukahara T, Tsukahara R, Yasuda S, Makarova N, Valentine WJ, Allison P, Yuan H, Baker DL, Li Z, Bittman R, et al. Different residues mediate recognition of 1-O-oleyllysophosphatidic acid and rosiglitazone in the ligand binding domain of peroxisome proliferator-activated receptor gamma. *J Biol Chem.* 2006; 281:3398–3407. [PubMed: 16321982]
- Tzamelis I, Fang H, Ollero M, Shi H, Hamm JK, Kievit P, Hollenberg AN, Flier JS. Regulated production of a peroxisome proliferator-activated receptor-gamma ligand during an early phase of adipocyte differentiation in 3T3-L1 adipocytes. *J Biol Chem.* 2004; 279:36093–36102. [PubMed: 15190061]
- Wanders RJ, Waterham HR. Biochemistry of mammalian peroxisomes revisited. *Annu Rev Biochem.* 2006; 75:295–332. [PubMed: 16756494]
- Wang YX. PPARs: diverse regulators in energy metabolism and metabolic diseases. *Cell Res.* 2010; 20:124–137. [PubMed: 20101262]
- Yang Q, Graham TE, Mody N, Preitner F, Peroni OD, Zabolotny JM, Kotani K, Quadro L, Kahn BB. Serum retinol binding protein 4 contributes to insulin resistance in obesity and type 2 diabetes. *Nature.* 2005; 436:356–362. [PubMed: 16034410]
- Yuan M, Konstantopoulos N, Lee J, Hansen L, Li ZW, Karin M, Shoelson SE. Reversal of obesity- and diet-induced insulin resistance with salicylates or targeted disruption of Ikkbeta. *Science.* 2001; 293:1673–1677. [PubMed: 11533494]

**HIGHLIGHTS**

- Fat-specific FAS KO mice have increased brite (brown in white) cells in subcutaneous adipose tissue and less diet-induced obesity.
- FAS knockdown in cultured cells blocks adipogenesis and PPAR $\gamma$  activation.
- FAS-dependent alkyl ether-linked phosphatidylcholines are associated with PPAR $\gamma$ .
- Knockdown of PexRAP, required for ether lipid synthesis, decreases diet-induced adiposity.

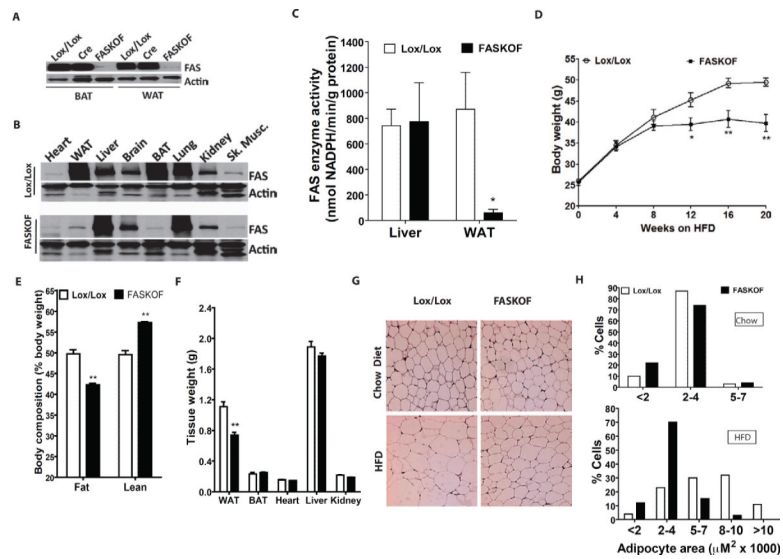


**Figure 1. Targeted Deletion of Adipose Tissue FAS Decreases Adiposity**

(A) FAS protein by Western blot in brown (BAT) and white (WAT) adipose tissue of Lox/Lox control (without Cre), adiponectin-Cre control (without floxed alleles), and FASKOF mice.

(B) Tissue distribution of FAS protein by Western blot. An apparent increased expression of hepatic FAS protein in FASKOF mice was not consistently observed.

(C) FAS enzyme activity assay. \* $P=0.031$ .  $N=4$ /genotype.

(D) Body weight of HFD-fed control and FASKOF male mice. Similar results were also obtained in two additional feeding experiments with different cohorts of male mice.

\* $P=0.03$ . \*\* $P=0.0068$  at 16 weeks, 0.0028 at 20 weeks.  $N=6-8$ /genotype. Additional data including females are provided in Table S1.

(E) MRI analysis of body composition in HFD-fed mice. \*\* $P<0.0001$ .  $N=6$ /genotype.

(F) Tissue weights of HFD-fed control and FASKOF mice. \*\* $P=0.005$ .  $N=6$ /genotype.

(G) Histologic appearance of WAT harvested from chow-fed or HFD-fed mice.

(H) Adipocyte size distribution determined with the NIH Image J program. Error bars in panels C–F represent SEM.

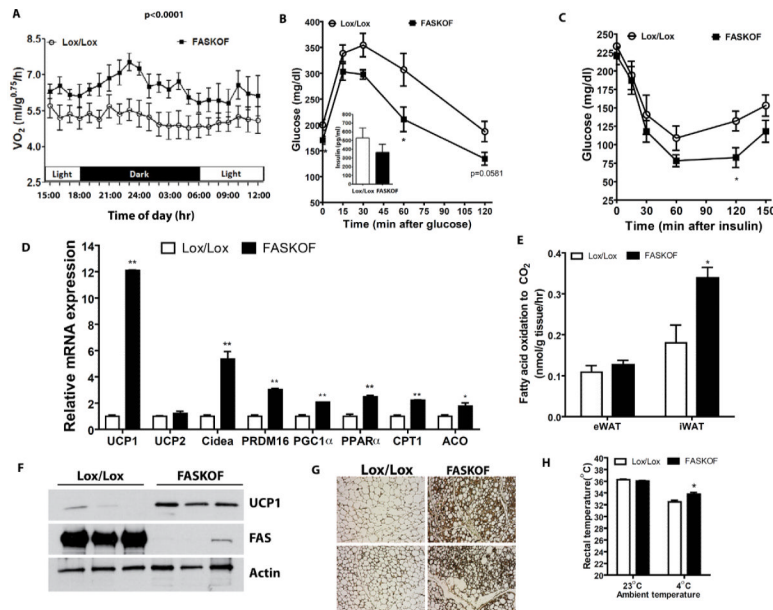


**Figure 2. Altered Metabolism in Mice with Adipose-specific Knockout of FAS**

(A) Oxygen consumption ( $VO_2$ ) by indirect calorimetry in HFD-fed mice. Indicated P value by ANOVA. N=8–10/genotype.

(B) Glucose tolerance testing in HFD-fed mice. P=0.0477 at 0 min, 0.0415 at 60 min. N=6–8/genotype. Serum insulin values at 30 min point shown in the inset.

(C) Insulin tolerance testing in the mice of panel B. \*P=0.039.

(D) RT-PCR analysis of gene expression in inguinal WAT of HFD-fed control and FASKOF male mice. Gene expression analysis in inguinal WAT of ZFD-fed mice is presented in Supplementary Figure 1H. \*\*P=<0.0001 for UCP1, 0.0017 for Cidea, 0.0001 for PRDM16, 0.0008 for PGC1 $\alpha$ , 0.0012 for PPAR $\alpha$ , and 0.0001 for CPT1; \*P=0.042 for ACO.

(E) Measurement of fatty acid oxidation in epididymal (eWAT) and inguinal (iWAT) fat of control and FASKOF mice fed HFD. \*P=0.0355 for HFD iWAT. N=3 animals/genotype for each diet.

(F) Western blot analysis in inguinal WAT of ZFD-fed control and FASKOF male mice. Each lane represents a separate mouse.

(G) Immunocytochemical analysis of UCP1 expression in inguinal WAT of ZFD-fed control and FASKOF mice. Images are from two separate mice per genotype.

(H) Rectal temperature of ZFD-fed control and FASKOF mice at room temperature (23°C) and after 1 hr exposure to 4°C. N=6–8 animals/genotype. \*P=0.011. Error bars in panels A–E and H represent SEM.



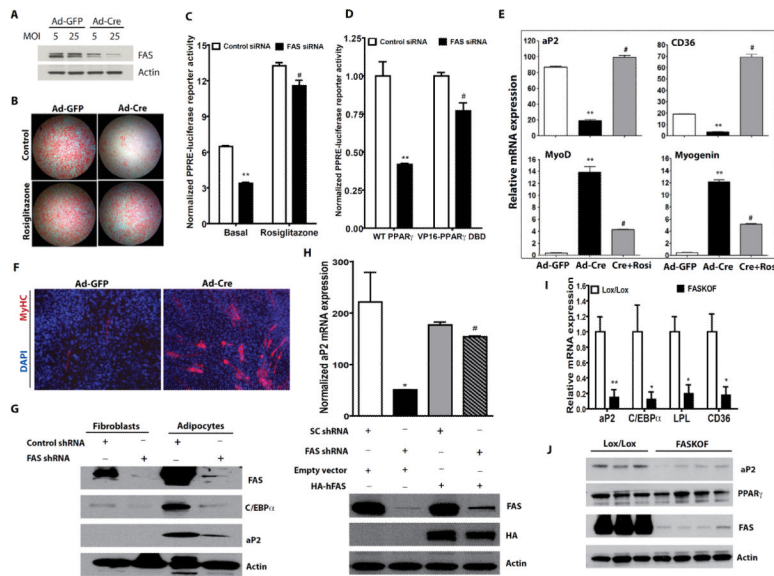


### Figure 3. FAS is Required for Adipogenesis and PPAR $\gamma$ Activation

(A) Western blot analysis of FAS knockdown in primary MEFs from FAS<sup>lox/lox</sup> mice treated with an adenovirus expressing GFP or Cre at the indicated multiplicity of infection (MOI).

(B) Oil red O staining of FAS<sup>lox/lox</sup> MEFs treated with Ad-GFP or Ad-Cre and differentiated to adipocytes in the presence or absence of rosiglitazone.

(C) HEK 293 cells treated with control or FAS siRNA were transfected with plasmids encoding PPRE-luciferase, *Renilla* luciferase and wild type PPAR $\gamma$  in the presence or absence of rosiglitazone. \*\**P*<0.0001 vs. control, #*P*<0.0001 vs. FAS siRNA basal. N=3/condition.

(D) HEK 293 cells treated with control or FAS siRNA were transfected with plasmids encoding PPRE-luciferase, *Renilla* luciferase and wild type PPAR $\gamma$  or VP16-PPAR $\gamma$  DBD (an N-terminal fragment of PPAR $\gamma$  encompassing the DNA binding domain fused to the VP16 transactivation domain). \*\**P*<0.0001 vs. control, #*P*<0.0001 vs. FAS siRNA/WT PPAR $\gamma$ . N=3/condition.

(E) RT-PCR analysis of gene expression in FAS-deficient (Ad-Cre-treated) or control (Ad-GFP-treated) MEFs subjected to the adipogenesis protocol. \*\*vs. Ad-GFP, *P*=0.0060 for aP2, 0.0010 for CD36, 0.0051 for MyoD, 0.0007 for Myogenin. #vs. Ad-Cre, *P*=0.0015 for aP2, 0.0013 for CD36, 0.0099 for MyoD, 0.0019 for Myogenin.

(F) FAS-deficient (Ad-Cre-treated) or control (Ad-GFP-treated) MEFs cultured to promote myogenesis and stained with a skeletal muscle myosin heavy chain antibody.

(G) Detection of proteins induced by PPAR $\gamma$  in 3T3-L1 fibroblasts and adipocytes treated with control or FAS shRNA.

(H) Restoration of PPAR $\gamma$  target gene expression with human FAS using 3T3-L1 adipocytes with endogenous knockdown of FAS. 3T3-L1 cells stably expressing retrovirally encoded human FAS were infected with a lentivirus expressing scrambled control (SC) or mouse FAS shRNA. The cells were induced to differentiate into adipocytes. The upper panel shows real-time PCR analysis of aP2 expression and the bottom panel shows a Western blot with antibodies against FAS, HA and actin. \**P*=0.0224 (vs. SC shRNA, empty vector). #*P*<0.0001 (vs. FAS shRNA, empty vector).

(I) RT-PCR analysis of gene expression in control and FASKOF gonadal WAT. \*\**P*=0.007. \**P*=0.0493 for C/EBP $\alpha$ , 0.010 for LPL, 0.039 for CD36. N=4/genotype.

(J) Western blot analysis in gonadal WAT of ZFD-fed control and FASKOF female mice. Each lane represents a separate mouse.

Error bars in panels C–E and H–I represent SEM.

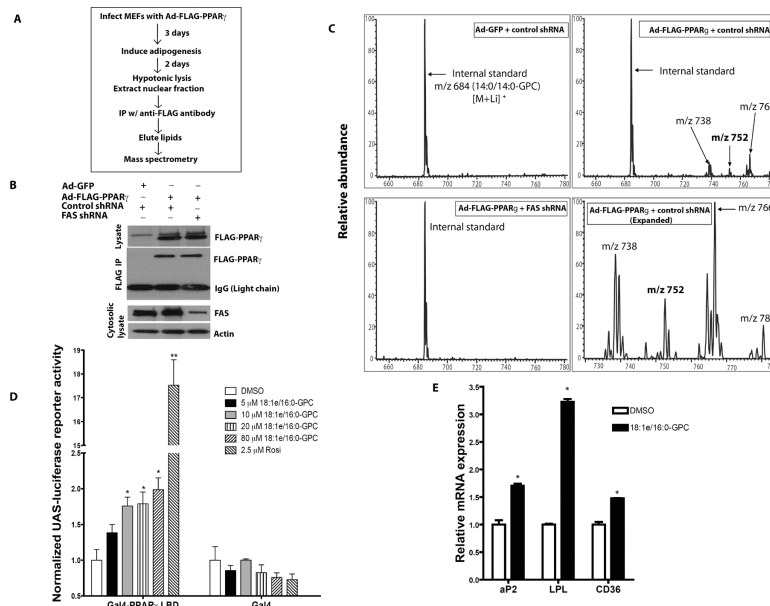


#### Figure 4. Isolation of FAS-dependent Diacyl and 1-O-alkyl Ether Phosphatidylcholine Species Associated with PPAR $\gamma$

(A) Strategy for detection of PPAR $\gamma$ -associated lipids.

(B) Detection of FLAG-PPAR $\gamma$  protein immunoprecipitated from adipocytes treated with control or FAS shRNA.

(C) Mass spectrometric analyses of [M+Li]<sup>+</sup> ions of glycerophosphocholine (GPC) lipids bound to FLAG-PPAR $\gamma$  or control protein (GFP) immunoprecipitated from control and FAS knockdown adipocytes. Ions of *m/z* 752 and 780 represent 1-O-alkyl GPC species.

(D) CV-1 cells were transfected with plasmids encoding UAS-luciferase, *Renilla* luciferase and Gal4-PPAR $\gamma$  LBD (a C-terminal fragment of PPAR $\gamma$  encompassing the ligand binding domain fused to the Gal4 DNA binding domain) or Gal4 alone. The cells were treated with 18:1e/16:0-GPC (corresponding to *m/z* 752 in panel C), rosiglitazone or DMSO. After 48 hrs, UAS-luciferase reporter activity was measured and normalized to *Renilla* luciferase reporter activity. \*\*P=0.0001. \*P=0.018 (10  $\mu$ M), 0.024 (20  $\mu$ M), 0.019 (80  $\mu$ M).

(E) 3T3-L1 cells were induced to differentiate in DMEM+10% FBS with supplemental dexamethasone, insulin and IBMX in the presence of 20  $\mu$ M 18:1e/16:0-GPC or DMSO. After 3 days, the cells were re-treated with the GPC in media containing supplemental insulin alone. The next day, the cells were harvested for RNA extraction and real-time PCR analysis. The data are representative of 3 separate experiments. \*P=0.0147 (aP2), 0.0006 (LPL), 0.0102 (CD36).

Error bars in panels D and E represent SEM.

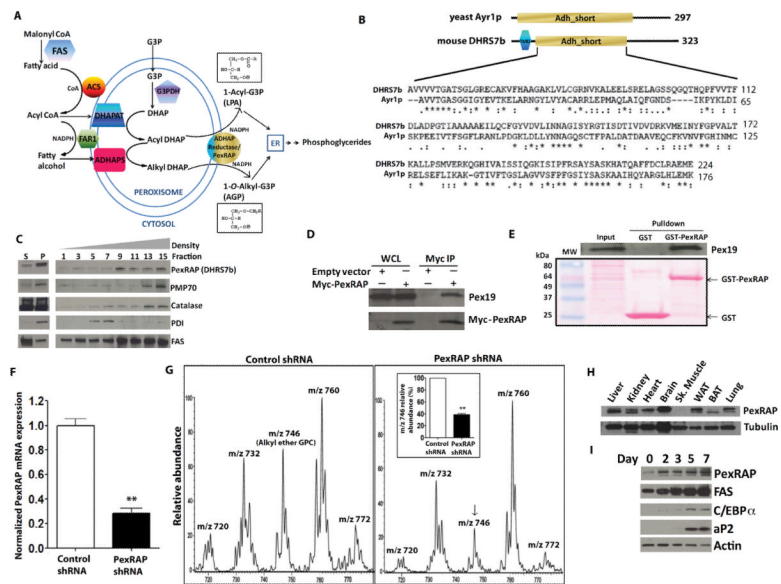


### Figure 5. Cloning and Characterization of the Terminal Component in the Mammalian Peroxisomal Ether Lipid Synthetic Pathway

(A) The peroxisomal acyl-DHAP pathway of lipid synthesis. FAS, fatty acid synthase; ACS, acyl CoA synthase; G3PDH, glycerol 3-phosphate dehydrogenase; DHAP, dihydroxyacetone phosphate; DHAPAT, DHAP acyltransferase; FAR1, fatty acyl CoA reductase 1; ADHAPS, alkyl DHAP synthase; ADHAP Reductase, acyl/alkyl DHAP reductase activity; LPA, lysophosphatidic acid; AGP, 1-*O*-alkyl glycerol 3-phosphate.

(B) Mouse Dhrs7b is homologous to yeast acyl DHAP reductase, Ayr1p. TMD, transmembrane domain; Adh\_short, short chain dehydrogenase/reductase domain.

(C) PexRAP (Peroxisomal Reductase Activating PPAR $\gamma$ , detected using anti-Dhrs7b antibody) is enriched in peroxisomal fractions isolated from 3T3-L1 adipocytes. S, supernatant; P, pellet after sedimentation.

(D) Pex19 co-immunoprecipitates with Myc-tagged PexRAP. WCL, whole cell lysates.

(E) Pex19 interacts with PexRAP in GST pull-down experiments using 3T3-L1 adipocytes.

(F) RT-PCR analysis of PexRAP expression with PexRAP knockdown in MEFs.

\*\* $P=0.0084$ .

(G) Mass spectrometric analyses of  $[M+H]^+$  ions of GPC lipids in MEFs after PexRAP knockdown. Quantification of the 1-*O*-alkyl ether GPC lipid peak at  $m/z$  746  $[M+H]^+$  (identical to the lithium adduct at  $m/z$  752 in Figure 4C) is shown in the inset. \*\* $P=0.0009$ .

(H) Mouse tissue distribution of PexRAP protein by Western blotting.

(I) Protein abundances of PexRAP and FAS increase prior to increases in C/EBP $\alpha$  and aP2 during differentiation of 3T3-L1 adipocytes.

Error bars in panels F and G (inset) represent SEM.

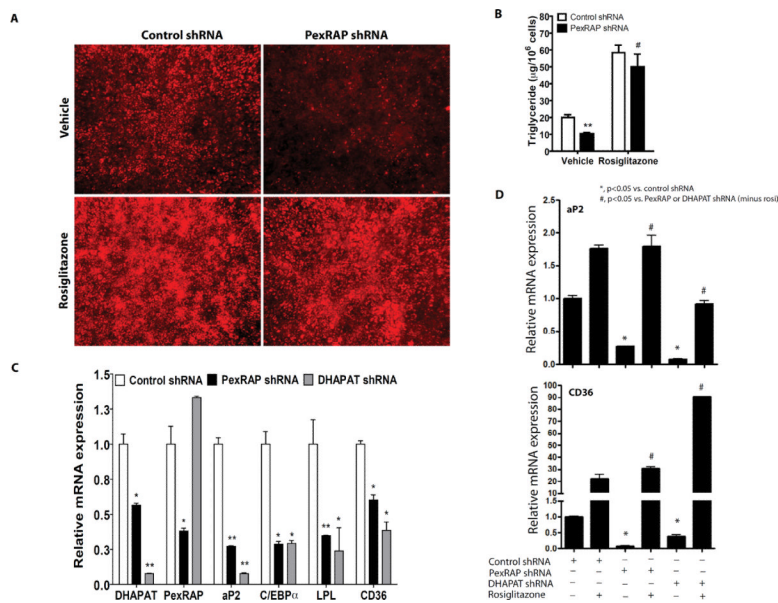


### Figure 6. PexRAP is Required for Adipogenesis and PPAR $\gamma$ Activation

(A) Nile red staining of 3T3-L1 adipocytes treated with control or PexRAP shRNA in the presence or absence of rosiglitazone.

(B) Triglyceride content for the cells of panel A. \*\*P=0.0066 vs. control, #P=0.0071 vs. PexRAP shRNA vehicle. N=3/condition.

(C) RT-PCR analysis of gene expression following PexRAP or DHAPAT knockdown. P vs. control: DHAPAT, \*0.0278, \*\*0.007; PexRAP, \*0.040; aP2, \*\*0.0060 for PexRAP shRNA and 0.0058 for DHAPAT shRNA; C/EBP $\alpha$ , \*0.0160 for PexRAP shRNA and 0.0165 for DHAPAT shRNA; LPL, \*\*0.0014, \*0.0450; CD36, \*0.0113 for PexRAP shRNA and 0.0132 for DHAPAT shRNA. N=3–5/condition.

(D) Rosiglitazone treatment rescues the effect of PexRAP or DHAPAT knockdown on PPAR $\gamma$  target gene expression. 3T3-L1 cells infected with lentivirus expressing control, PexRAP, or DHAPAT shRNA were induced to differentiate into adipocytes and then treated with 2.5  $\mu$ M rosiglitazone. Expression of PPAR $\gamma$  target genes was analyzed by quantitative RT-PCR. For aP2, exact P values from left to right= 0.0038, 0.0119, 0.0024, 0.0032. For CD36, P values= 0.0022, 0.0015, 0.0110, <0.0001.

Error bars in panels B–D represent SEM.

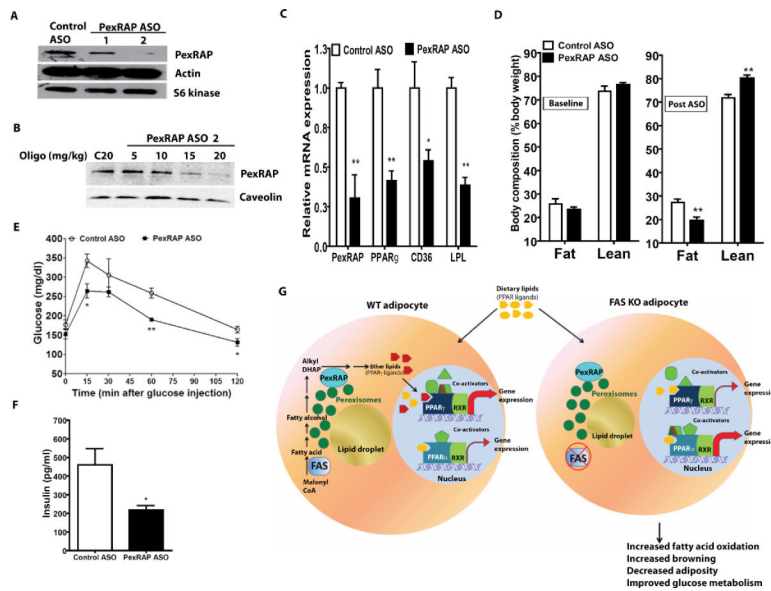


### Figure 7. Knockdown of PexRAP in Mice Alters Body Composition and Metabolism

(A) PexRAP knockdown using antisense oligonucleotides (ASOs) in Hepa1-6 cells.

(B) Western blot analysis using epididymal WAT of C57BL/6J mice treated intraperitoneally with the indicated doses of control or PexRAP ASO twice a week for 3 weeks.

(C) RT-PCR analysis of epididymal WAT expression following ASO treatment. P vs. control: PexRAP  $**0.0078$ ; PPAR $\gamma$   $**0.0051$ ; CD36  $*0.0420$ ; LPL  $**0.0030$ . N=4/condition.

(D) Body composition by MRI following 4 weeks of HFD feeding (baseline) and after 3.5 weeks of ASO treatment while still eating a HFD.  $**P=0.0098$  for fat,  $0.0071$  for lean. N=4/condition.

(E) Glucose tolerance testing in HFD-fed mice following ASO treatment.  $*P=0.0220$  at 15 min. and  $0.0434$  at 120 min.  $**p=0.0019$ .

(F) Insulin levels at the 30 min point from panel E.  $*P=0.0363$ .

(G) Models of PPAR $\gamma$  and PPAR $\alpha$  gene expression in WT and FAS-deficient adipocytes.

Error bars in panels C–F represent SEM.